11th PAMIR International Conference - Fundamental and Applied MHD
July 1 – 5, 2019, Reims, France

A NEW TYPE OF DOUBLE-DIFFUSIVE HELICAL MAGNETOROTATIONAL INSTABILITY IN ROTATIONAL FLOWS WITH POSITIVE SHEAR

G. MAMATSASHVILI[1,2*], *F. STEFANI*[2], *R. HOLLERBACH*[3], *G. RÜDIGER*[4]

[1]*Niels Bohr International Academy, Niels Bohr Institute, Blegdamsvej 17, 2100 Copenhagen, Denmark*
[2]*Helmholtz-Zentrum Dresden - Rossendorf, Bautzner Landstr. 400, 01328 Dresden, Germany*
[3]*Department of Applied Mathematics, University of Leeds, Leeds LS2 9JT, U.K.*
[4]*Leibniz-Institut für Astrophysik Potsdam, An der Sternwarte 16, D-14482 Potsdam, Germany*

*Corresponding author: george.mamatsashvili@nbi.ku.dk

Abstract: We revealed a novel type of axisymmetric magnetorotational instability in viscous and resistive rotating flows with radially increasing angular velocity, or positive shear, exposed to a helical magnetic field. It operates for a broad range of positive shear, provided that magnetic Prandtl number is not unity. This instability can play an important role in the magnetic activity of the equatorial parts of the solar tachocline, where the shear of differential rotation is positive.

Key words: Magnetorotational Instabilities, liquid metals

1. Introduction The standard version of magnetorotational instability (SMRI) with axial magnetic field [1] as well as its "relatives" in viscous and resistive flows – azimuthal MRI (AMRI, with a purely azimuthal field [2]) and the helical MRI (HMRI, with combined axial and azimuthal fields [3]) – have been investigated theoretically in great detail in the case of flows with radially decreasing angular velocity and increasing specific angular momentum, which are hydrodynamically stable. AMRI and HMRI have also been detected in experiments [4, 5], while a solid experimental evidence of SMRI is still missing, despite promising first efforts [6].

By contrast, much less attention is dedicated to flows with radially increasing angular velocity, because up to now such flows have been regarded as strongly stable, even in the presence of magnetic fields. However, for high enough Reynolds numbers $Re = O(10^6)$, they can exhibit non-axisymmetric linear instabilities, as recently shown in [7]. Besides this hydrodynamic instability, there exists a special type of AMRI at much lower Reynolds numbers but sufficiently high positive shear [8]. Yet, the latter limitation makes this so-called *Super-AMRI* astrophysically less relevant. One of the few positive shear domains is a part of the tachocline within $\pm 30^\circ$ about the solar equator [9]. However, even there, the shear expressed in terms of Rossby number $Ro = r(2\Omega)^{-1}d\Omega/dr$ is about 0.7, much less than the so-called *upper Liu limit* (ULL) $Ro_{ULL} = 2(1+\sqrt{2}) \approx 4.83$ [10] needed for Super-AMRI.

Given the general affinity between AMRI and HMRI [11], one might anticipate a similar result also for *Super-HMRI*. However, as we show below, using Wentzel-Kramers-Brillouin (WKB) short-wavelength approach, there exists in fact a new type of axisymmetric HMRI which can operate for arbitrary positive shear. The only requirements are the presence of both axial and azimuthal field components, and magnetic Prandtl number different from both zero (the inductionless limit) and from unity. These conditions are fulfilled in the solar tachocline, where this new instability can potentially play a key role in its magnetic activity.

2. Presentation of the problem Consider a Taylor-Couette flow of an incompressible, conducting fluid which rotates with angular velocity profile $\Omega(r)$ between two cylinders with radii r_i and r_o. The imposed helical magnetic field has a constant axial, B_{0z}, and a radially-dependent, current-free azimuthal components, $B_{0\phi}(r) = \beta B_{0z} r_o/r$, where β characterizes field's helicity. We investigate the linear stability of this equilibrium to axisymmetric perturbations of the form $\propto \exp(\gamma t + \mathrm{i}k_r r + \mathrm{i}k_z z)$, where γ is the (complex) frequency and k_r and k_z are the radial and axial wavenumbers. The resulting dispersion relation can be expressed as a fourth-order polynomial [11],

$$\gamma^4 + a_1\gamma^3 + a_2\gamma^2 + (a_3 + \mathrm{i}b_3)\gamma + a_4 + \mathrm{i}b_4 = 0, \tag{1}$$

with the coefficients

$$a_1 = 2k^2 Re^{-1}(1 + Pm^{-1}),$$
$$a_2 = 2(k_z^2 + 2\alpha^2\beta^2)Ha^2Re^{-2}Pm^{-1} + 4\alpha^2(1 + Ro) + k^4Re^{-2}\left(1 + 4Pm^{-1} + Pm^{-2}\right),$$
$$a_3 = 8(1 + Ro)\alpha^2k^2Re^{-1}Pm^{-1} + 2k^2Re^{-3}Pm^{-1}\left(1 + Pm^{-1}\right)[k^4 + (k_z^2 + 2\alpha^2\beta^2)Ha^2],$$
$$b_3 = -8\alpha^2\beta k_z Ha^2Re^{-2}Pm^{-1},$$

$$a_4 = 4\alpha^2k^4Pm^{-2}\left[(1 + Ro)Re^{-2} + \beta^2Ha^2Re^{-4}\right] + 4\alpha^2k_z^2RoHa^2Re^{-2}Pm^{-1} + Re^{-4}Pm^{-2}\left(k_z^2Ha^2 + k^4\right)^2,$$

$$b_4 = 4k_z^3\beta\left[Ro\left(1 - Pm^{-1}\right) - 2Pm^{-1}\right]Ha^2Re^{-3}Pm^{-1}.$$

The roots with a positive real part, $\mathrm{Re}(\gamma) > 0$, indicate instability. Here, γ is normalized by Ω_o, and the wavenumbers by r_o^{-1}. The other parameters are: $\alpha = k_z/k$, where $k = (k_r^2 + k_z^2)^{1/2}$ is the total wavenumber; the Reynolds and magnetic Reynolds numbers are $Re = \Omega_o r_o^2/\nu$ and $Rm = \Omega_o r_o^2/\eta$, and their ratio, the magnetic Prandtl number $Pm = \nu/\eta = Rm/Re$, where ν is viscosity and η resistivity; the Hartmann number $Ha = B_{0z}r_o/\sqrt{\mu_0\rho_0\nu\eta}$, characterizing the imposed axial field, where ρ_0 is the (constant) density and μ_0 the magnetic permeability.

We focus specifically on positive Rossby numbers (shear), $Ro > 0$, so that the flow is stable both hydrodynamically and against SMRI with purely axial field (i.e., $\beta = 0$) [11]. As for the dependence on β, as long as $\beta \neq 0$, it follows from Eq. (1) that β can be removed by re-scaling the wavenumbers, Hartmann and Reynolds numbers as $k_z/\beta \to k_z$, $k/\beta \to k$, $Re/\beta^2 \to Re$, $Ha/\beta \to Ha$, which does not change these coefficients and hence the eigenfrequencies. Without loss of generality, we set $\beta = 1$.

In the inductionless case, $Pm \to 0$, Eq. (1) can be solved analytically [11]. For positive and relatively large $Ro > Ro_{ULL}$, one of the roots always has a positive real part,

$$\mathrm{Re}(\gamma) = \sqrt{2X + 2\sqrt{X^2 + Y^2}} - (k_z^2 + 2\alpha^2\beta^2)Ha^2Re^{-1}k^{-2} - Rek^{-2}, \tag{2}$$

where

$$X = \alpha^2\beta^2(\alpha^2\beta^2 + k_z^2)Ha^4Re^{-2}k^{-4} - \alpha^2(1 + Ro),$$
$$Y = \beta\alpha^2k_z(2 + Ro)Ha^2Re^{-1}k^{-2},$$

which is the growth rate of HMRI operating at positive shear, i.e. Super-HMRI. *Our primary goal is to demonstrate that besides this Super-HMRI at larger positive shear, Eq. (1) also gives an entirely new type of dissipation-induced, or double-diffusive instability at nonzero Pm.*

Figure 1a presents the growth rate $\mathrm{Re}(\gamma)$ versus the axial wavenumber, following from a numerical solution of Eq. (1) at finite but very small $Pm = 10^{-6}$, alongside the inductionless

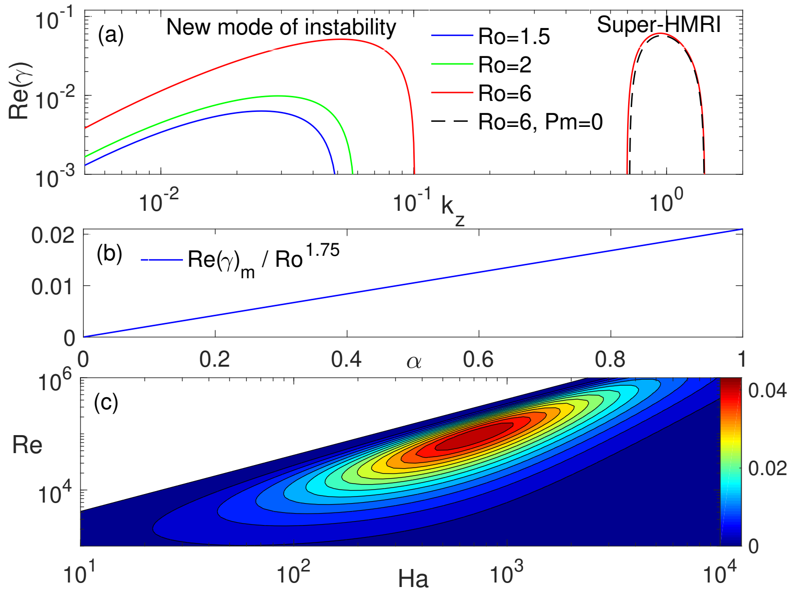

Figure 1: Panel (a) plots the growth rate Re(γ) vs. k_z, at $Ha = 90$, $Re = 8\cdot10^3$, $\alpha = 0.71$ ($k_r = k_z$), and $Pm = 10^{-6}$, for various $Ro = 1.5,\ 2,\ 6$ alongside the inductionless solution (2) for $Ro = 6$ (black dashed line). The new instability branch is at smaller k_z and finite Pm, for all Ro, whereas Super-HMRI branch at larger k_z exists only for $Ro = 6 > Ro_{ULL}$, but persists in the inductionless case. For this Pm, panel (b) shows the growth rate of the instability, maximized over k_z, Ha and Re and normalized by $Ro^{1.75}$, vs. α, while panel (c) shows this growth rate maximized over k_z and α, in (Ha, Re)-plane at $Ro = 1.5$.

solution (2) for given Ha and Re. We consider Rossby numbers lower, $Ro = 1.5, 2$, and larger, $Ro = 6$, than Ro_{ULL}. We can clearly identify two distinct instability regimes. The first one is located at small k_z and occurs at finite Pm both for $Ro < Ro_{ULL}$ and $Ro > Ro_{ULL}$, i.e. it is independent of the Liu limit, but vanishes for $Pm \to 0$ at given Hartmann and Reynolds numbers. By contrast, the second one, Super-HMRI, is located at larger k_z, occurs only for $Ro > Ro_{ULL}$, and tends to the inductionless solution as $Pm \to 0$.

The first instability branch is a new dissipation-induced mode at positive shear, which needs *both* finite viscosity and resistivity. As shown below, it does not operate near $Pm = 1$, that is, it is double-diffusive, operating for both small and large Pm. As for all MRI-type instabilities, the present one is supplied by shear flow energy, since the imposed field is current-free, thereby excluding current-induced instabilities. Like the familiar HMRI at negative shear, energy is extracted from the flow to the perturbations due to the coupling between meridional circulation and azimuthal field perturbations brought about by the imposed azimuthal field. Super-HMRI, existing for $Ro > Ro_{ULL}$ is also new and interesting, but is not covered here.

To explore the behavior of the new instability further, we first vary α, Hartmann and Reynolds numbers. The growth rate, maximized over the last two numbers and k_z, increases linearly with α and scales as $\propto Ro^{1.75}$ (Fig. 1b), while its dependence on Ha and Re, when maximized over k_z and α is shown in Fig. 1c at $Pm = 10^{-6}$ and $Ro = 1.5 < Ro_{ULL}$ (where Super-HMRI is absent). The unstable area is localized, with the growth rate decreasing for both small and large Ha and Re, implying that the instability, being double-diffusive, exists at finite viscosity and resistivity. The overall structure in (Ha, Re)-plane does not change qualitatively at other Pm and Ro; the unstable area is always localized, but moves up to larger Ha and Re with decreasing Pm. The maximum growth rate, γ_m, is reached at $Ha_m = 665$ and $Re_m = 8.64\cdot10^4$ in Fig. 1c; as noted above, for a given γ these values can be rescaled to larger β.

Next we look at how the growth rate varies with Pm again at fixed $Ro = 1.5 < Ro_{ULL}$, so that Super-HMRI is excluded. Figure 2 shows the growth rate γ_m, maximized over k_z, Ha and

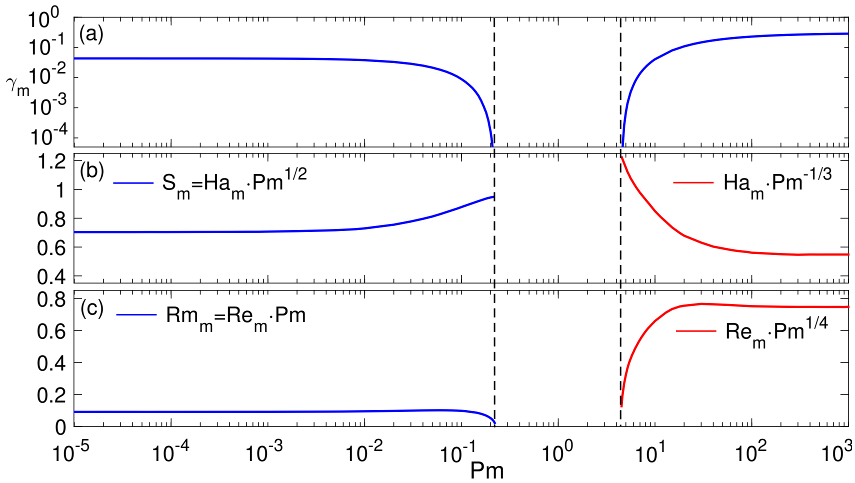

Figure 2: Panel (a) presents the growth rate γ_m, optimized over k_z, Ha and Re, vs. Pm, at fixed $Ro = 1.5$ and $\alpha = 1$. Panels (b) and (c) show the corresponding Ha_m and Re_m, respectively. For both $Pm \ll 1$ and $Pm \gg 1$, γ_m approaches constant values. The Hartmann and Reynolds numbers scale as $Ha_m \propto Pm^{-1/2}$ and $Re_m \propto Pm^{-1}$ for $Pm \ll 1$, and as $Ha_m \propto Pm^{1/3}$ and $Re_m \propto Pm^{-1/4}$ for $Pm \gg 1$. Panels (b) and (c) are compensated by these factors to more clearly show these scalings. The dashed lines are at $Pm_{c1} = 0.223$ and $Pm_{c2} = 4.46$, marking the stable region around $Pm = O(1)$.

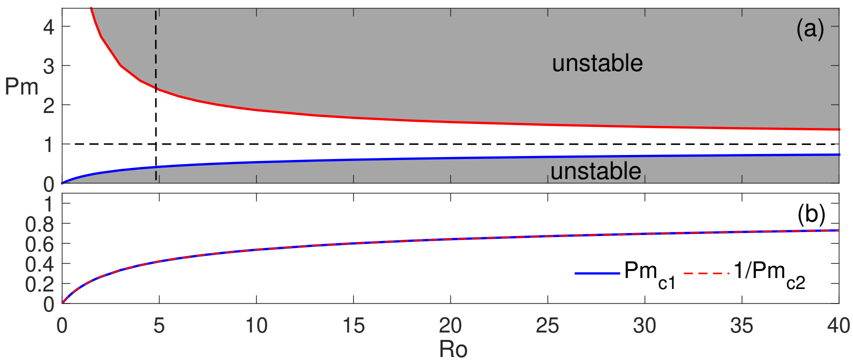

Figure 3: Panel (a) plots the lower (Pm_{c1}, blue) and upper (Pm_{c2}, red) margins of the instability vs. Ro. Panel (b) shows that these marginal curves are related by $Pm_{c1} = 1/Pm_{c2}$. The vertical dashed line in (a) marks the Liu limit $Ro_{ULL} = 4.83$, showing that the instability is not affected by this limit.

Re, as a function of Pm as well as the corresponding Ha_m and Re_m at which this maximum growth is reached. We see that for $Pm \lesssim 10^{-2}$, the growth rate is essentially constant, $\gamma_m = 0.043$, while Ha_m and Re_m increase with decreasing Pm as power-laws, with $Ha_m \propto Pm^{-1/2}$ and $Re_m \propto Pm^{-1}$. That is, in this small-Pm regime the instability is better characterized by Lundquist, $S_m = Ha_m \cdot Pm^{1/2} = 0.7$, and magnetic Reynolds, $Rm_m = Re_m \cdot Pm = 0.091$, numbers and is hence independent of Pm, as is SMRI, meaning that this new instability does not exist in the inductionless limit, which implies $S, Rm \to 0$ if Ha and Re remain finite.

With increasing Pm, beyond $Pm \sim 0.01$, γ_m steeply decreases, and eventually the instability vanishes at the first critical point $Pm_{c1} = 0.223$, with corresponding $Ha_m = 2.018$, $Re_m = 0.071$, and critical wavenumber $k_{zm} = 0.0024$. It emerges again for larger Pm at the second critical point $Pm_{c2} = 4.46$, with $Ha_m = 2$, $Re_m = 0.046$, and $k_{zm} = 0.005$. Further increasing Pm, for $Pm \gtrsim 10$, γ_m finally reaches a constant value of 0.29. The corresponding Hartmann and Reynolds numbers again follow power-laws, $Ha_m \propto Pm^{1/3}$ and $Re_m \propto Pm^{-1/4}$. So, this new instability exists over a broad range of magnetic Prandtl numbers, provided that viscosity ν and resistivity η differ, so that $Pm = 1$ is avoided, and instead $Pm < Pm_{c1} < 1$ or $Pm > Pm_{c2} > 1$.

Figure 3a shows the unstable regions in (Ro, Pm)-plane. For all Ro, the two marginal ($\gamma_m = 0$) curves satisfy $Pm_{c1} < 1$ and $Pm_{c2} > 1$, and are related by $Pm_{c1}Pm_{c2} = 1$, as seen in Fig. 3b. For high shear ($Ro \to \infty$), the stable interval about $Pm = 1$ becomes increasingly narrow, so most Pm values are unstable, whereas for $Ro \to 0$, the stable interval broadens to encompass all Pm. This is because the shear is the only energy source (just as it is for SMRI, AMRI, and HMRI) and hence there can be no instability at all for $Ro = 0$, which is a solid-body rotation. Note also that Pm_{c1} and Pm_{c2} stability curves are unaffected by the Liu limit at $Ro_{ULL} = 4.83$, and the instability exists also for $Ro < Ro_{ULL}$.

3. Conclusions We have revealed and analyzed a new type of double-diffusive HMRI which is able to destabilize rotating flows with arbitrary positive shear, including $0 < Ro < Ro_{ULL}$ where magnetorotational instabilities were thought to be absent. The only requirements are that $Pm \neq 1$, and the imposed magnetic field must consist of both axial and azimuthal components. Both these conditions are fulfilled in the equatorial parts of the solar tachocline, for which this new type of HMRI may have important consequences. Specifically, it can revive the idea of a subcritical solar dynamo. Its axisymmetric ($m = 0$) nature can overcome the difficulties that arise [12] in getting the so-called Tayler-Spruit dynamo [13] to form a closed dynamo loop from the joint action of the $m = 1$ Tayler instability and the $m = 0$ Ω-effect.

Acknowledgements. This project has received funding from the European Union's Horizon 2020 research and innovation programme under the Marie Skłodowska– Curie Grant Agreement No. 795158 and the ERC Advanced Grant Agreement No. 787544

REFERENCES

[1]. E.P. VELIKHOV, *JETP* ,**9**, 995 (1959); S. CHANDRASEKHAR, *Proce. Natl. Acad. Sci.*, **46**, 253 (1960)

[2]. R. HOLLERBACH, V. TEELUCK, G. RÜDIGER, *Phys. Rev. Lett.*, **104**, 044502 (2010)

[3]. R. HOLLERBACH, G. RÜDIGER, *Phys. Rev. Lett.*, **95**, 124501 (2005)

[4]. M. SEILMAYER et al., *Phys. Rev. Lett.*, **13**, 024504 (2014)

[5]. F. STEFANI et al., *Phys. Rev. Lett.*, **97**, 184502 (2006); F. STEFANI et al., *Phys. Rev. E.*, **80**, 066303 (2009)

[6]. D.R. SISAN et al., *Phys. Rev. Lett.*, **93**, 114502 (2004); M.D. NORNBERG et al., *Phys. Rev. Lett.*, **104**, 074501 (2010)

[7]. K. DEGUCHI, *Phys. Rev. E.*, **95**, 021102(R) (2017)

[8]. F. STEFANI, O. KIRILLOV, *Phys. Rev. E*, **92**, 051001 (2015); G. RÜDIGER et al., *Phys. Fluids*, **28**, 014105 (2016); G. RÜDIGER et al., *J. Plasma Phys.*, **84**, 735840101 (2018)

[9]. K. PARFREY, K. MENOU, *Astrophys. J. Lett.*, **667**, L207 (2007)

[10]. W. LIU et al. *Phys. Rev. E*, **74**, 056302 (2006)

[11]. O.N. KIRILLOV, F. STEFANI, Y. FUKUMOTO, *Astrophys. J.*, **756**, 83 (2012); O.N. KIRILLOV, F. STEFANI, Y. FUKUMOTO, *J. Fluid Mech.*, **760**, 591 (2014); G. MAMATSASHVILI, F. STEFANI, *Phys. Rev. E.*, **94**, 051203(R) (2016)

[12]. J.-P. ZAHN, A.S. BRUN, S. MATHIS, *Astron. Astrophys.*, **474**, 145 (2007)

[13]. H. SPRUIT, *Astron. Astrophys.*, **381**, 923 (2002)